the compensation is achieved for one value of x, it is not good enough for a rather different value of x. Consequently, even the present assumption is contradicted.

The extension of the above argument for three and more regions of $f(i)$ values is obvious. We may, therefore, conclude that the requirement that the McLaurin coefficients form a smooth function of i is a very strong one. It implies that all plausible representations of function $F(x)$, which are subject to this requirement, yield sets of McLaurin coefficients which differ only insignificantly among themselves. The only exception are coefficients of those terms, which do not contribute significantly to the value of $F(x)$ at any value of $x \in \langle a,b \rangle$.

References and Notes

(1) H. Tompa, "Polymer Solutions", Academic Press, New York, N.Y., 1956.
(2) H. Yamakawa, "Modern Theory of Polymer Solutions", Harper and Row, New York, N.Y., 1971.
(3) C. Domb, J. Gillis, and G. Wilmers, *Proc. Phys. Soc., London*, **85**, 625 (1965).
(4) F. T. Wall and F. T. Hioe, *J. Phys. Chem.*, **74**, 4410 (1970).
(5) F. T. Wall and J. Erpenbeck, *J. Chem. Phys.*, **30**, 634 (1959).
(6) F. T. Wall, *J. Chem. Phys.*, **63**, 3713 (1975).
(7) F. L. McCrackin, J. Mazur, and Ch. M. Guttman, *Macromolecules*, **6**, 859 (1973).
(8) P. J. Flory, "Principles of Polymer Chemistry", Cornell University Press, Ithaca, N.Y., 1953.
(9) P. Munk and M. E. Halbrook, *Macromolecules*, **9**, 441 (1976).
(10) C. Tanford, "Physical Chemistry of Macromolecules", Wiley, New York, N.Y., 1961.
(11) E. Slagowski, B. Tsai, and D. McIntyre, *Macromolecules*, **9**, 687 (1976).
(12) A. Dondos and H. Benoit, *Makromol. Chem.*, **133**, 119 (1970).
(13) M. Gordon, J. A. Torkington, and S. B. Ross-Murphy, *Macromolecules*, **10**, 1090 (1977).
(14) **Note Added in Proof:** After this paper was submitted for publication, Gordon et al.[13] published a paper using a novel approach for handling the intersegmental contacts. Their method is based on the random walk on the lattice with intersections allowed. The intersections are considered to be local violations of the lattice condition; they represent the contacts. The authors have shown that for this model in the limit for long walks the function $W_n(m,i)$ approaches Gaussian form. The position of the maximum is a linear function of the length of the chain m. Such a behavior is in qualitative agreement with the results presented in our paper; this is apparent from our Figure 2. However, the Gaussian function, if plotted in coordinates of Figure 2, would exhibit a parabolic (i.e., symmetrical) form. Our lines exhibit assymetry which, while decreasing with increasing m, is still very pronounced for $m = 3000$. The discrepancy may be caused by our (arbitrary) choice of the function $\bar{i}(m,x)$, eq 35 and 36. However, the difference may also indicate that the limit of long walks must be applied with caution; it is possible that it is applicable only far beyond the region of the interest of a polymer chemist. (Gordon et al.[13] discuss the correction for shorter chains as effecting only the width of the Gaussian curve and not its Gaussian character.) Another difference may be related to the previous one: Gordon et al. predict that the change of the interaction parameter and of the coil expansion is accompanied by a relatively small change in the number of contacts. Our model predicts a massive change, cf. Figure 3. We are grateful to Professor Gordon for directing our attention toward his recent work.

Polymerization of Methyl Methacrylate Photoinitiated by 4,4′-Bis(N,N-diethylamino)benzophenone. 1

V. D. McGinniss,*[1a] T. Provder, C. Kuo, and A. Gallopo[1b]

Glidden Coatings and Resins, Division of SCM Corporation, Strongsville, Ohio 44136, and Montclair State College, Upper Montclair, New Jersey.

Received September 26, 1977

ABSTRACT: Polymerization of methyl methacrylate (MMA) photoinitiated by 4,4′-bis(N,N-diethylamino)benzophenone (DEABP) was shown to have unusual kinetic behavior attributable to primary radical termination reactions. This deviation from normal kinetic orders in light intensity, photoinitiator, and monomer concentrations qualitatively parallels observed concentration effects on quantum yield for the photochemical disappearance of Michler's ketone in cyclohexane. Increasing the DEABP concentration, beyond certain limits, lowers the rate of photopolymerization for MMA analogous with lowering of the quantum yield for disappearance of Michler's ketone with increasing concentrations of reactant. Molecular weights of the photopolymerized samples are significantly lower than for thermally initiated polymerizations using azodiisobutyronitrile (VAZO-64) as initiator. It is also shown that DEABP (ground state) does not influence the rate of polymerization or the molecular weight distribution of VAZO-64 thermally initiated polymerization of methyl methacrylate. Multiple detector GPC/IR/UV examination of thermally polymerized MMA showed no fragments of DEABP attached to the polymer backbone thus eliminating the possibility of growing polymer radical chain transfer to the ground state photoinitiator. Analysis of the photopolymerized MMA by GPC/IR/UV multiple detection does show photoinitiator or photoproduct fragments attached to the polymer backbone and accounts for the observed lowering of molecular weights (initiation as well as primary radical termination). Broadening of the molecular weight distribution (monomodal to almost bimodal) for the photopolymerized MMA between narrow DEABP concentration ranges indicated a change in photoinitiation mechanism. Drastic solvent effects (nonpolar–polar) were observed for the photoinitiated polymerization of MMA using DEABP initiator. Polymer formation decreased as the polarity and reactivity of the solvent–MMA mixtures were changed from benzene (polymer formed), cyclohexane (little polymer formation), and methanol (no polymer formed). These results are attributable to the decrease in the quantum yield for intersystem crossing efficiency (ϕ_{st}) of aminoaromatic ketones (Michler's ketone) as the polarity and reactivity of the solvent changes. Reaction mechanisms and kinetic schemes, consistent with the experimental observations, are presented and discussed.

In the past 10 years, an intensive industrial effort has been directed toward pollution-free coatings. The area of ultraviolet-initiated polymerization (photoinitiated cure) has grown considerably, especially with the commercialization of ultraviolet curable inks and wood coatings. The rapid increase of patent literature on new photoinitiators and radiation curable coating systems is strong indication that photopolymerization will be a very important pollution-free curing process in the near future.

The use of 4,4′-bis(N,N-dimethylamino)benzophenone (Michler's ketone) and benzophenone as photoinitiators for the photopolymerization of vinyl unsaturation have been disclosed in the recent patent literature.[1-4] The photophysical processes involved or associated with the photochemistry of

0024-9297/78/2211-0393$01.00/0

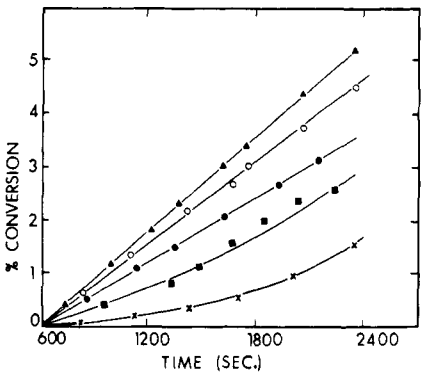

Figure 1. Photopolymerization of MMA at 30 °C with 4,4′-bis(diethylamino)benzophenone (DEABP) photoinitiator; [DEABP] =: (●) 0.05×10^{-2} M; (○) 0.5×10^{-2} M; (△) 1×10^{-2} M; (□) 3×10^{-2} M; (X) 6×10^{-2} M.

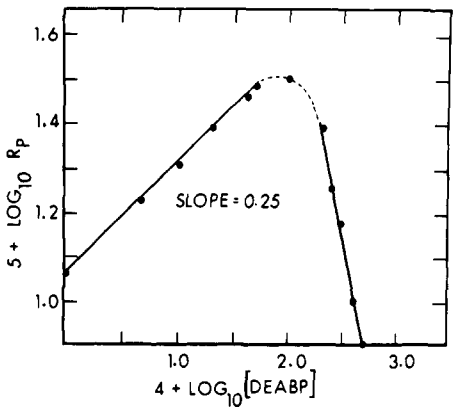

Figure 2. Plot of log R_p against log [DEABP] for the photopolymerization of MMA at 30 °C.

benzophenone and Michler's ketone have also been reported by several authors.[5-11]

In this paper we present details of the kinetics and mechanisms of reactions associated with the photoinitiated polymerization of methyl methacrylate, in nitrogen, sensitized by 4,4′-bis(*N*,*N*-diethylamino)benzophenone (DEABP).

Experimental Section

Materials. The removal of inhibitor from methyl methacrylate was accomplished through washing three times with 5% aqueous sodium hydroxide solution followed by washing with deionized water. This inhibitor free monomer was dried over anhydrous calcium chloride and then distilled under reduced pressure. Only the middle fraction of the distillate was collected and used for the photopolymerization experiments.

Aldrich (99+% gold label) 4,4′-bis(diethylamino)benzophenone (DEABP), mp 94.5–95 °C, was used without further purification as the photoinitiator. Azodiisobutyronitrile (AIBN) (Eastman Kodak) was recrystallized four times from absolute ethanol, mp 102 °C [VAZO-64 (DuPont) AIBN].

Benzophenone derivatives were obtained from Aldrich or Eastman Kodak and were used without further purification (98+% purity as received).

Eastman Kodak benzophenone and benzhydrol were recrystallized twice from 40–60 and 60–80 °C petroleum ether to give crystals with respective melting points of 48 and 68°. Solvents were spectrograde materials and were used without further purification.

Methods. Light Source and Rates of Polymerization. The light source used was a high-pressure 450 W, quartz, mercury-vapor lamp (Hanovia) which was placed in a water cooled, quartz, immersion well (Ace Glass Co.). The immersion well contained a Pyrex sleeve and the entire assembly was housed in a 30 ± 0.05 °C constant temperature bath. The outside of this immersion well was entirely covered with an aluminum sleeve except for a narrow window that allowed the ultraviolet irradiation to enter a 13-mL dilatometer reaction cell. Rates of polymerization were followed by conventional dilatometric techniques.[12]

Calibration of Light Source. Changes in intensity of energy output of the UV lamp were followed by the technique of Block, Ledwith, and Taylor[12] where the photopolymerization of MMA with AIBN was used as a light calibration standard. Initial light intensity was determined through benzophenone/benzhydrol actinometry ($I_0 = 8 \times 10^{16}$ quanta/s).[13]

Spectra. Qualitative visible spectra of photoproduct production was determined on a Bausch & Lomb Spectronic 20 spectrophotometer.

Molecular Weights. The molecular weights and molecular weight distributions (MWD) were determined with a multiple detector gel permeation chromatograph (GPC) system using infrared (IR) and ultraviolet (UV) detectors.[14,15]

The instrument was operated at 23 °C at a flow rate of 1.47 mL/min with Burdick and Jackson distilled in glass chloroform as the mobile phase. The sample column bank consisted of five Styragel™ columns with nominal porosity designations 10^6, 3×10^5, 10^4, 10^3, 250 Å and had a plate count of 400 plates/ft and a resolution factor of 1.74.[16] Primary molecular weight calibration curves were obtained from polystyrene standards available from ArRo Labs, Pressure Chemical Co., and Duke Standards Co. The secondary molecular weight calibration curve for poly(methyl methacrylate) (PMMA) was obtained via the hydrodynamic volume approach[17,18] using an expression first derived by Coll and Prusinowski[19]

$$\log M_x = \left(\frac{1}{1+\epsilon_x}\right) \log (K_s/K_x) + \left(\frac{1+\epsilon_s}{1+\epsilon_x}\right) f_s(V) \qquad (1)$$

where s and x denote the polystyrene polymer standard and PMMA samples of interest, respectively. The numerical values chosen for K_s, K_x, ϵ_s, and ϵ_x are 7.16×10^{-5}, 6×10^{-5}, 0.76, and 0.79, respectively.[20,21] Molecular weight averages were calculated by previously described methods.[18]

Number and weight average molecular weights ($\overline{M}_n$ and $\overline{M}_w$) calculated from the PMMA calibration curve were corrected for instrument spreading effects. The correction equations used were those developed by Provder and Rosen[22] by solving Tung's[23] equation via the "Method of Molecular Weight Averages" used in conjunction with a linear molecular weight calibration curve. The corrected molecular weight avarages $\overline{M}_n(c)$ and $\overline{M}_w(c)$ are expressed in terms of the uncorrected GPC molecular weight averages $\overline{M}_n(u)$ and $\overline{M}_w(u)$ and given by the expressions

$$\overline{M}_n(c) = \overline{M}_n(u)\{X_1(1 + X_2)\} \qquad (2)$$

$$\overline{M}_w(c) = \overline{M}_w(u)/\{X_1(1 - X_2)\} \qquad (3)$$

where X_1 and X_2 are measures of axial dispersion and chromatogram skewing, respectively.

The parameters X_1 and X_2 are determined from polystyrene standards using the following equations

$$X_1 = \tfrac{1}{2}\left\{\frac{\overline{M}_n(t)}{\overline{M}_n(u)} + \frac{\overline{M}_w(u)}{\overline{M}_w(t)}\right\} \qquad (4)$$

$$X_2 = \{(\Phi - 1)/(\Phi + 1)\} \qquad (5)$$

$$\Phi = \left(\frac{\overline{M}_n(t)}{\overline{M}_n(u)}\right)\left(\frac{\overline{M}_w(t)}{\overline{M}_w(u)}\right) \qquad (6)$$

where $\overline{M}_n(u)$ and $\overline{M}_w(u)$ are the uncorrected GPC molecular weight averages and $\overline{M}_n(t)$ and $\overline{M}_w(t)$ are the "true" or experimentally observed molecular weight averages. The molecular weights of photopolymerized PMMA were corrected for instrument spreading using eq 2 and 3 and plots of X_1 and X_2 vs. peak retention volume.

Results

Preliminary studies of the polymerization of methyl methacrylate (MMA) photoinitiated by 4,4′-bis(diethylamino)benzophenone (DEABP) showed that as the concentration of photoinitiator increases beyond 1×10^{-2} M, the slope of the percent conversion curves or rate of polymerization decreases. At higher concentrations of photoinitiator, long wavelength absorption photoproducts or side reactions accompany this decrease in rate of polymerization.[24]

Rates of Polymerization. The percent conversion curves of monomer (MMA) to polymer (PMMA) as a function of exposure time for various concentrations of DEABP are plotted in Figure 1. The rates of photopolymerization (R_p) for each concentration of DEABP were calculated from the initial

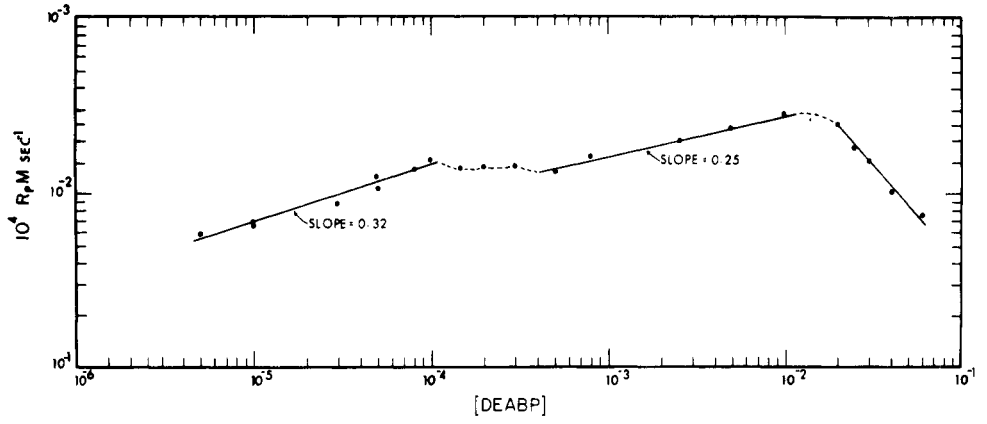

Figure 3. Plot of log R_p against log [DEABP] for the photopolymerization of MMA at 30 °C; [DEABP] = 0.5×10^{-5} M to 10×10^{-5} M and 1.5×10^{-4} M to 50×10^{-4} M.

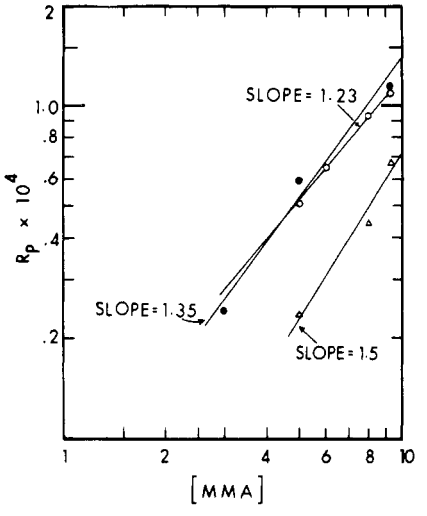

Figure 4. Variation of [MMA] on initial rates of polymerization (R_p) at [DEABP] = 1×10^{-5} M (△), 5×10^{-4} M (●), and 3×10^{-2} M (○).

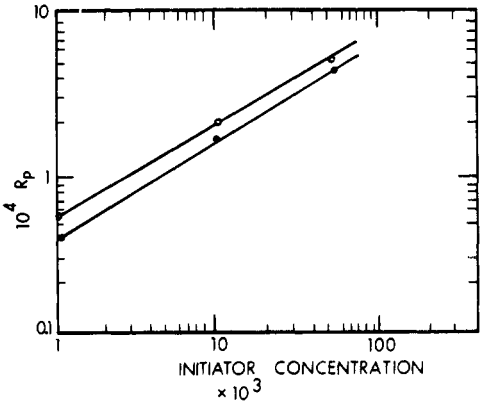

Figure 5. Plot of the rate of polymerization (R_p) vs. concentrations of [VAZO-64] (●) and [VAZO-64 + $DEABP_{(ground\ state)}$] (○) for thermally polymerized PMMA.

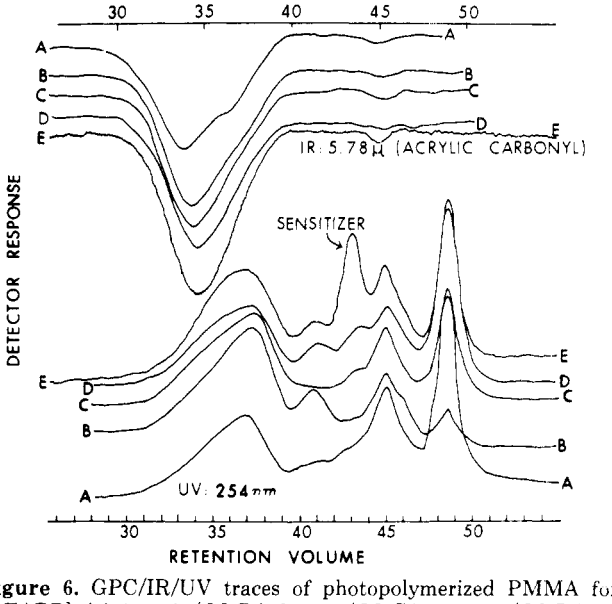

Figure 6. GPC/IR/UV traces of photopolymerized PMMA for [DEABP]: A is 5×10^{-4} M, B is 8×10^{-4} M, C is 12×10^{-4} M, D is 25×10^{-4} M, E is 50×10^{-4} M.

linear slopes of Figure 1 and are shown in Figure 2. The complete concentration range dependence of DEABP on the rates of photopolymerization (R_p) is given in Figure 3. The dependence of these rates of photopolymerization on the order of initiatior concentration is found to be 0.32 at [DEABP] = 0.5×10^{-5} to 1×10^{-4} M down to 0.25 at [DEABP] = $1.5\text{–}50 \times 10^{-4}$ M. The effect of varying [MMA] on initial rates of polymerization of MMA at [DEABP] = 1×10^{-5}, 5×10^{-4}, and 3×10^{-2} M is given in Figure 4. The dependence of rates of photopolymerization on the order of monomer concentration varies between 1.5, 1.35, and 1.23 (1.36 average) for [DEABP] = 1×10^{-5}, 5×10^{-4}, and 3×10^{-2} M, respectively. The rates of polymerization dependence on the order of light intensity varied between 0.54, 0.47, and 0.34 (0.44 average) for [DEABP] = 1×10^{-5}, 5×10^{-4}, and 3×10^{-2} M (deviations in order of light intensity could be caused by internal screening effects since $\epsilon = 40\,700$ M^{-1} cm^{-1} for DEABP).[11]

In order to see if the photoinitiator has any effect on the rate of polymerization of a ground state reaction, a thermal polymerization of MMA with azodiisobutyronitrile (VAZO-64) was carried out in the presence and absence of DEABP. The plot of log R_p vs. log [VAZO-64] is linear as is the plot of log R_p vs. [Vazo-64 + $DEABP_{(ground\ state)}$]. The order in initiator concentration for both cases is 0.5 (Figure 5). This is in exact agreement with the literature value for polymerizations of MMA using VAZO-64 as the only thermal initiator.[25]

Molecular Weights. The multiple detector GPC/IR/UV system separates the photopolymerization reaction products into polymer fractions, initiator fragments, and polymer fractions containing initiation or termination chromophors. In Figure 6 is a composite GPC/IR/UV chromatogram for the photopolymerized PMMA samples as a function of initiator concentration. Several points can be made about the GPC/UV traces: (1) the sensitizer fragments are chemically bound to the polymer chain ends; (2) a greater number of sensitizer fragments reside in the lower molecular weight regions; (3) a

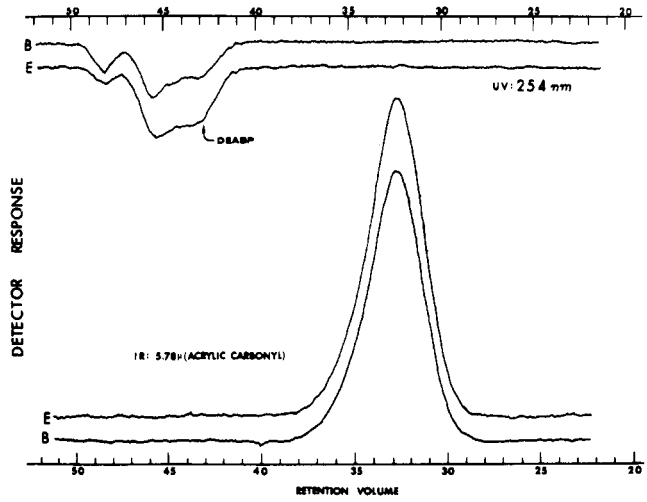

Figure 7. GPC/IR/UV traces of thermally polymerized PMMA in the presence of VAZO-64 and $DEABP_{(ground\ state)}$.

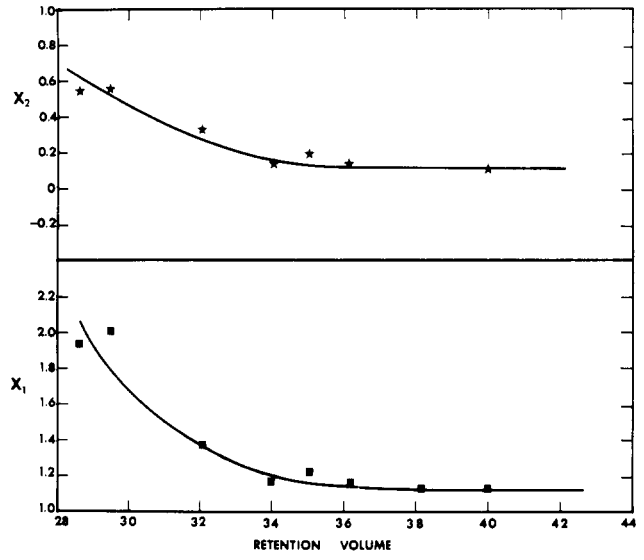

Figure 8. Plots of X_1 and X_2 vs. retention volume for the GPC/IR detector.

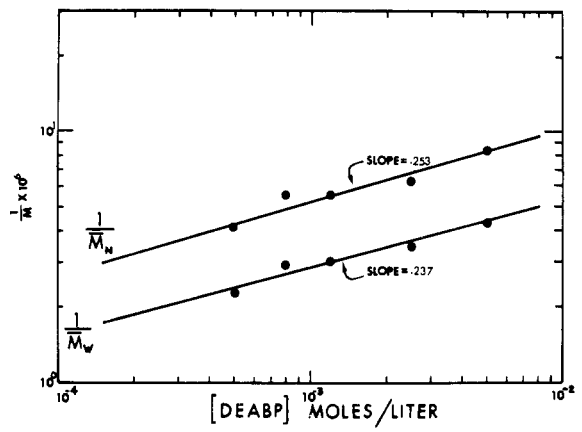

Figure 9. Dependence of molecular weight on the concentration of DEABP for the photopolymerized MMA.

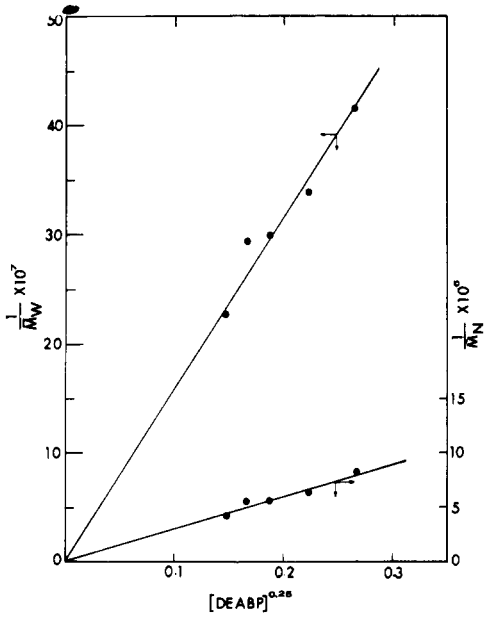

Figure 10. Plot of reciprocal molecular weights vs. $[DEABP]^{0.25}$.

considerable amount of free sensitizer can be detected as shown at retention volume ~43 counts; and (4) the other peaks beyond counts 40 could be due to unidentified photoproducts. Examination of the GPC/IR traces indicates that the most obvious difference observable is that the shape of the GPC/IR traces changes from a symmetrical single peak to a double peak when the concentration of the initiator decreases. Also, the position of the peak shifts to a lower retention volume.

In Figure 7 is a composite GPC/IR/UV chromatogram for the thermally polymerized PMMA with added DEABP at different concentration levels.

It is seen from the GPC/UV traces that for the ground state reaction, no DEABP fragments are bound to the polymer chains. The concentration of initiator has no effect on the shape of the IR traces even for the samples with the highest concentration.

In Figure 8 are shown the axial dispersion (X_1) and skewing (X_2) correction factors plotted vs. retention volume for the GPC column setting based on polystyrene standards. Corrected values for the molecular weight averages of PMMA using these parameters (X_1, X_2) are given in Table I. These results indicate that the instrument spreading correction did not have a significant effect on $\overline{M}_w$ for photopolymerized PMMA but did raise the values of $\overline{M}_n$. Therefore, the polydispersity index was greatly reduced.

The same effect was observed for the thermally polymerized PMMA shown in Table II. The interesting point here is that the average molecular weight for these samples is the same as that of the control samples within the experimental error. Light-scattering measurements on selected PMMA samples showed that the light-scattering molecular weights are in agreement with the instrument spreading corrected GPC values within experimental error. These data further illustrated the consistency of the hydrodynamic volume/instrument spreading correction approach for obtaining PMMA molecular weights.

Table III compares the molecular weights of photopolymerized and thermally polymerized PMMA. The addition of DEABP to the ground state reaction did not affect the molecular weight. The polydispersity index is close to 1.50 as the theory would predict for termination by combination. In the case of photopolymerized PMMA, the molecular weight decreases as the concentration of DEABP increases. Also the polydispersity index is broader than that of the ground state reaction. Therefore, it seems to indicate that the termination mechanism is by combination with some transfer reactions.[26]

An interesting feature of the GPC/IR trace (Figure 6) is that at DEABP concentrations below 1×10^{-4} M and above 8×10^{-4} M the molecular weight peaks are symmetrical. At

Table I
Molecular Weight Statistics for Photopolymerized PMMA

Photosensitizer concn × 10^2 mol/L	$\overline{M}_n$(u)[a] × 10^{-3}	$\overline{M}_n$(c)[b] × 10^{-3}	$\overline{M}_w$(u) × 10^{-3}	$\overline{M}_w$(c) × 10^{-3}	P(u)	P(c)
0.05	167	245	445	442	2.67	1.80
0.08	116	177	340	337	2.93	1.92
0.12	123	181	335	334	2.73	1.85
0.25	115	164	304	296	2.64	180
0.50	89.9	120	260	240	2.90	2.00

[a]The $\overline{M}_n$(u), $\overline{M}_w$(u), and P(u) are those values prior to the correction for the instrument spreading. [b]The $\overline{M}_n$(c), $\overline{M}_w$(c), and P(c) are the corrected values.

Table II
Effect of Instrument Spreading Correction on the Molecular Weight Statistics of Thermally Polymerized PMMA at 60 °C (with Photosensitizer and 2.23 × 10^{-2} M VAZO-64 Added)

Photosensitizer concn × 10^2 mol/L	$\overline{M}_n$(u)[a] × 10^{-3}	$\overline{M}_n$(c)[b] × 10^{-3}	$\overline{M}_w$(u) × 10^{-3}	$\overline{M}_w$(c) × 10^{-3}	P(u)	P(c)
0.05	160	240	447	442	2.79	1.78
0.08	164	266	453	455	2.76	1.71
0.12	183	283	451	446	2.46	1.58
0.25	173	268	436	431	2.52	1.61
0.50	190	301	473	460	2.49	1.55
Av	174	272	452	447	2.60	1.65
0 (control)	182	286	455	450	2.50	1.57

[a]The $\overline{M}_n$(u), $\overline{M}_w$(u), and P(u) are those values prior to the correction for the instrument spreading. [b] The $\overline{M}_n$(c), $\overline{M}_w$(c), and P(c) are the corrected values.

Table III
Comparison of the Molecular Weight Statistics between Thermally Polymerized and Photopolymerized PMMA

Photosensitizer concn × 10^2 mol/L	$\overline{M}_n$(thermal) × 10^{-3}	$\overline{M}_n$(photo) × 10^{-3}	$\overline{M}_w$(thermal) × 10^{-3}	$\overline{M}_w$(photo) × 10^{-3}	P(thermal)	P(photo)
0.05	240	245	442	445	1.78	1.80
0.08	266	177	455	340	1.71	1.92
0.12	283	181	446	335	1.58	1.85
0.25	268	164	431	304	1.61	1.80
0.50	301	120	460	260	1.55	2.00
Av	272		447			

Table IV
Molecular Weight Statistics of Photopolymerized PMMA

Photosensitizer concn × 10^5 mol/L	$\overline{M}_n$(u)[a] × 10^{-3}	$\overline{M}_n$(c)[b] × 10^{-3}	$\overline{M}_w$(u) × 10^{-3}	$\overline{M}_w$(c) × 10^{-3}	P(u)	P(c)
1	264	449	687	687	2.60	1.53
3	216	348	537	544	2.48	1.56
5	150	230	283	381	2.55	1.66
8	125	189	362	359	2.90	1.89

[a]The $\overline{M}_n$(u), $\overline{M}_w$(u), and P(u) are those values prior to the correction for the instrument spreading. [b]The $\overline{M}_n$(c), $\overline{M}_w$(c), and P(c) are the corrected values.

DEABP concentrations of 1.5×10^{-4} M up to 8×10^{-4} M the molecular weight peaks are broad and almost bimodal or contain unresolved shoulders. This apparent broadening of the molecular weight peaks indicates a change in mechanism associated with unique concentration dependence of the initiator for the photopolymerization process. The rates of polymerization dependence on initiator approach ideal order (0.5) at lower concentrations of DEABP where $R_p \propto [\text{DEABP}]^{0.32}$ when [DEABP] $\simeq 10^{-5}$ M. At higher concentrations $R_p \propto [\text{DEABP}]^{0.25}$ when [DEABP] $\simeq 10^{-4}$ M.

The dependence of the molecular weight averages $\overline{M}_n$ and $\overline{M}_w$ on the concentration of DEABP in the range $1.5–50 \times 10^{-4}$ M for the photopolymerized PMMA is plotted in Figure 9 and shown in Table I. The average of the slopes for these plots is 0.25 within experimental error and Figure 10 shows the linear relationship when the reciprocal molecular weight averages are plotted against $[\text{DEABP}]^{0.25}$. This is in excellent agreement with the R_p dependence on $[\text{DEABP}]^{0.25}$ for [DEABP0 , 5×10^{-4}–50×10^{-4} M.

The dependence of the molecular weight averages, $\overline{M}_n$ and $\overline{M}_w$, on the concentration of DEABP in the range 0.5×10^{-5} to 1×10^{-4} M for the photopolymerized PMMA is shown in Table IV. In this concentration range the relationship between the reciprocal molecular weight and [DEABP] is linear with respect to $[\text{DEABP}]^{0.41}$ for $\overline{M}_n$ and is linear with respect to $[\text{DEABP}]^{0.33}$ for $\overline{M}_w$. The 0.33 order in [DEABP] from the $\overline{M}_w$ results is closely in accord with the 0.32 order in [DEABP] from the kinetic results

Discussion

The experimentally determined order of reaction with respect to photoinitiator concentration dependence, monomer, and light intensity for the photopolymerization of MMA

are

$$R_p \propto I_0^{0.3 \text{ to } 0.5}[\text{DEABP}]^{0.2 \text{ to } 0.4}[\text{MMA}]^{1.2 \text{ to } 1.3} \quad (7)$$

This deviation from normal photopolymerization kinetic orders might be attributable to primary radical or photoproduct termination interactions with growing polymer radicals. Monomer orders greater than 1 (1 to 1.5) have been reported for MMA as well as orders in initiator less than 0.5 for certain acrylate and methacrylate esters.[27] These deviations from normal kinetic orders were attributable to primary initiator radical recombination mechanisms, primary radical termination with growing polymer radicals, or formation of relatively inactive transfer radicals.[28] The following kinetic schemes have been proposed to account for higher orders in MMA:

$$R_p = K_1[M]^{3/2}[I]^{1/2}/(1 + K_2[M])^{1/2} \quad (8)$$

$$R_p = \frac{K_p[M]K_1^{1/2}[I]^{1/2}}{K_t^{1/2}}\left\{\frac{K_3[M]}{K_2 + K_3[M]}\right\}^{1/2} \quad (9)$$

These expressions, however, do not account for rate dependence on lower initiation exponents.[29]

The low kinetic order in initiator is also consistent with primary initiator radical competition for monomer and other deactivation pathways.

$$R\cdot + M \rightarrow M\cdot \quad (10)$$

$$M\cdot + M \rightarrow P\cdot \quad (11)$$

$$R\cdot + R\cdot \rightarrow \text{absorbing photoproducts} \quad (12)$$

$$R\cdot + \text{photoproducts} \rightarrow \text{termination} \quad (13)$$

$$R\cdot + P\cdot \rightarrow \text{termination} \quad (14)$$

$$P\cdot + \text{photoproducts} \rightarrow \text{termination} \quad (15)$$

Variations in light intensity orders are consistent with screen effects due to photoproduct formation. The photoproducts and primary radical fragments absorb light in the same area as the photoinitiator (DEABP) and could lead to internal quenching of the reaction rate.[29]

In order to explain observed kinetic orders for the photopolymerization of MMA with DEABP it is necessary first to understand the photochemistry associated with aminoaromatic ketones.

Photochemistry of Michler's Ketone Derivatives. Aminoaromatic carbonyl compounds such as Michler's ketone (MK) and DEABP are ideally suited as photoinitiators in that they have large extinction coefficients, charge-transfer states, and relatively long triplet lifetimes in solution.[24,30,31] Michler's ketone derivatives are also unique in that they can photoproduce two different types of free-radical intermediates $R_1\cdot$ and $R_2\cdot$. The detailed kinetic scheme has been worked out for MK and by analogy applies to DEABP. This complete kinetic scheme is shown below.

$$\left.\begin{aligned} &\text{DEABP}^0 \xrightarrow{h\nu} \\ &\quad \text{DEABP}^1 \quad \text{(excitation)} \quad I_{abs} \end{aligned}\right\} \quad (16)$$

$$\left.\begin{aligned} &\text{DEABP}^1 \xrightarrow{K_{st}} \\ &\quad \text{DEABP}^3 \quad \begin{matrix}\text{(intersystem}\\ \text{crossing)}\end{matrix} \quad [\text{DEABP}^1]K_{st} \end{aligned}\right\} I_{abs}\,\phi_{st} \quad (17)$$

$$\text{DEABP}^3 \xrightarrow{K_d} \text{DEABP}^0 \quad \begin{matrix}\text{(triplet}\\ \text{deactivation)}\end{matrix} \quad [\text{DEABP}^3]K_d \quad (18)$$

$$\text{DEABP}^3 + \text{DEABP}^0 \xrightarrow{K_e} [\text{triplet eximer}] \quad [\text{DEABP}^3][\text{DEABP}^0]K_e \quad (19)$$

$$[\text{triplet eximer}] \xrightarrow{K_d'} 2\text{DEABP}^0 \quad [\text{triplet eximer}]K_d' \quad (20)$$

$$[\text{triplet eximer}] \xrightarrow{K_r} R_1\cdot + R_2\cdot \text{ (bimolecular reaction and free-radical formation)} \quad [\text{triplet eximer}]K_r \quad (21)$$

Where

$R_1\cdot =$ 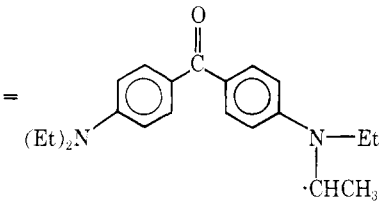 (22)

$R_2\cdot =$ 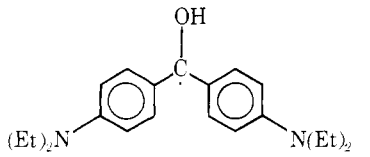

$R_1\cdot + R_2\cdot \xrightarrow{K_{t_1}}$ 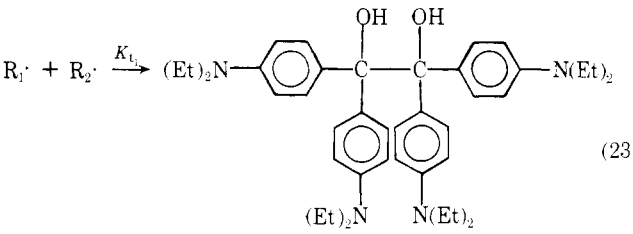 (23)

(pinacol) I

$R_1\cdot + R_2\cdot \xrightarrow{K_{t_2}}$ 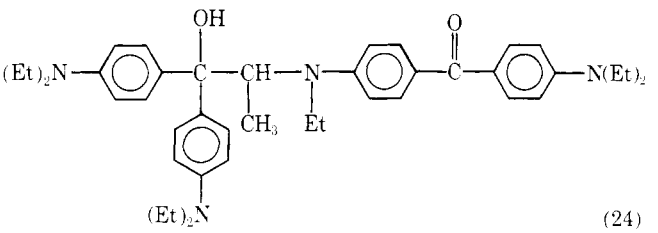 (24)

(photoproduct) II

$$\text{DEABP}^3 + \underset{\text{(solvent)}}{\text{ZH}} \xrightarrow{K_s} R_2\cdot + Z\cdot \text{ (solvent reaction)} \quad [\text{DEABP}^3][\text{ZH}]K_s \quad (25)$$

$$\text{DEABP}^3 + \underset{\text{(quencher)}}{\text{Q}} \xrightarrow{K_q} \text{DEABP}^0 \text{ (quenching)} \quad [\text{DEABP}^3][\text{Q}]K_q \quad (26)$$

The overall reaction for rate of disappearance of DEABP is

$$-d[\text{DEABP}^0]/dt = I_{abs}\phi_{st} - [\text{DEABP}^3]K_d + [\text{DEABP}^3][\text{DEABP}^0]K_e - [\text{DEABP}^3][\text{Q}]K_q \quad (27)$$

and the rate of formation and destruction of [DEABP³] is

$$d[\text{DEABP}^3]/dt = I_{abs}\phi_{st} - [\text{DEABP}^3]K_d - [\text{DEABP}^3][\text{DEABP}^0]K_e - [\text{DEABP}^3][\text{ZH}]K_s - [\text{DEABP}^3][\text{Q}]K_q \quad (28)$$

Assuming steady state conditions for [DEABP³] leads to

$$[\text{DEABP}^3] = I_{abs}\phi_{st}/(K_d + [\text{DEABP}^0]K_e + [\text{ZH}]K_s + [\text{Q}]K_q) \quad (29)$$

The rate of formation and destruction of the triplet eximer is

$$\text{d[triplet eximer]}/dt = [\text{DEABP}^3][\text{DEABP}^0]K_e - [\text{triplet eximer}]K_d' - [\text{triplet eximer}]K_r \quad (30)$$

Assuming steady state conditions for triplet eximer leads to

$$[\text{triplet eximer}] = [\text{DEABP}^3][\text{DEABP}^0]K_e/(K_r + K_d') \quad (31)$$

Substitution of eq 29 into eq 31 yields

$$[\text{triplet eximer}] = \frac{I_{abs}\phi_{st}[\text{DEABP}^0]K_e}{(K_r + K_d')(K_d + [\text{DEABP}^0]K_e + [\text{ZH}]K_s + [\text{Q}]K_q)} \quad (32)$$

The rate of primary radical formation in the absence of monomer is given by

$$\text{d[R}_1\cdot \text{ and R}_2\cdot\text{]}/dt = [\text{triplet eximer}]K_r + [\text{DEABP}^3][\text{ZH}]K_s - 2[\text{R}_2\cdot]^2Kt_1 - [\text{R}_1\cdot][\text{R}_2\cdot]Kt_2 \quad (33)$$

$$\frac{\text{d[R}_1\cdot \text{ and R}_2\cdot\text{]}}{dt} = \frac{I_{abs}\phi_{st}[\text{DEABP}^0]K_eK_r}{(K_d + [\text{DEABP}^0]K_e + [\text{ZH}]K_s + [\text{Q}]K_q)(K_r + K_d')} + \frac{I_{abs}\phi_{st}[\text{ZH}]K_s}{K_d + [\text{DEABP}^0]K_e + [\text{ZH}]K_s + [\text{Q}]K_q} - 2[\text{R}_2\cdot]^2Kt_1 - [\text{R}_1\cdot][\text{R}_2\cdot]Kt_2 \quad (34)$$

Assuming steady state conditions leads to

$$[\text{R}_2\cdot]^2 + \frac{[\text{R}_1\cdot][\text{R}_2\cdot]Kt_2}{2Kt_1} = \frac{I_{abs}\phi_{st}}{2Kt_1(K_d + [\text{DEABP}^0]K_e + [\text{ZH}]K_s + [\text{Q}]K_q)} \times \left\{\frac{[\text{DEABP}^0]K_eK_r}{(K_r + K_d')} + [\text{ZH}]K_s\right\} \quad (35)$$

The rate of formation of radical $R_1\cdot$ is given by

$$\text{d[R}_1\cdot\text{]}/dt = [\text{triplet eximer}]K_r - [\text{R}_1\cdot][\text{R}_2\cdot]Kt_2 \quad (36)$$

Then applying steady state conditions for $[R_1\cdot]$ and using eq 32 leads to

$$[\text{R}_1\cdot] = \frac{I_{abs}\phi_{st}K_r[\text{DEABP}^0]K_e}{[\text{R}_2\cdot]Kt_2\{(K_d + [\text{DEABP}^0]K_e, + [\text{ZH}]K_s + [\text{Q}]K_q)(K_r + K_d')\}} \quad (37)$$

Expressing eq 35 in terms of $[R_2\cdot]$ by using eq 37 in conjunction with eq 35 leads to the following expression for $[R_2\cdot]$

$$[\text{R}_2\cdot] = \left(\frac{[\text{ZH}]K_sI_{abs}\phi_{st}}{2Kt_1(K_d + [\text{DEABP}^0]K_e + [\text{ZH}]K_s + [\text{Q}]K_q)}\right)^{1/2} \quad (38)$$

Therefore, the rate of pinacol formation in eq 23 is given by

$$\text{rate of formation d(I)}/dt = \frac{[\text{ZH}]K_sI_{abs}\phi_{st}}{K_d + [\text{DEABP}^0]K_e + [\text{ZH}]K_s + [\text{Q}]K_q} \quad (39)$$

Then the rate of photoproduct (II) formation in eq (24) is given by

$$\text{rate of formation d(II)}/dt = \frac{I_{abs}\phi_{st}K_rK_e[\text{DEABP}^0]}{(K_d + [\text{DEABP}^0]K_e + [\text{ZH}]K_s + [\text{Q}]K_q)(K_r + K_d')} \quad (40)$$

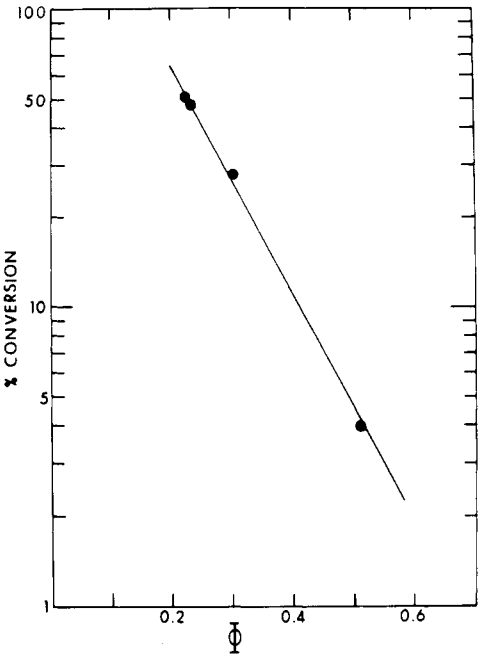

Figure 11. Plot of dependence of quantum yield (Φ) for disappearance of Michler's ketone (MK) as a function of percent conversion. (Data taken from ref 31.)

Quantum yields for photoproducts I and II are given by

$$\Phi_{(I)} = \frac{\text{rate of pinacol (I) formation without added quencher } [\text{Q}]K_q}{I_{abs}\phi_{st}} \quad (41)$$

$$\Phi_{(II)} = \frac{\text{rate of photoproduct (II) formation neglecting } [\text{Q}]K_q}{I_{abs}\phi_{st}} \quad (42)$$

where $I_{abs} = I_0[\text{DEABP}^0]\epsilon$ and ϕ_{st} for Michler's ketone (MK) is solvent dependent and can vary between 0.08 and 1.[31]

The photochemical disappearance of aminoaromatic ketones (MK and by analogy DEABP) in solvents with formation of photoproducts similar to I and II strongly depends on initial starting concentrations, the polarity or chemical structure of the solvent, and extent of reaction. Michler's ketone was found to have significant changes in quantum yield for destruction of initial starting material (cyclohexane solvent) as a function of initial concentration. These variations were $\phi \simeq 0.4$, $[\text{MK}^0] = 5 \times 10^{-6}$–$5 \times 10^{-5}$ M, $\phi = 0.2$, $[\text{MK}^0] = 5 \times 10^{-4}$ M, and $\phi = 0.1$, $[\text{MK}^0] > 5 \times 10^{-4}$ M. These quantum yields are consistent with the change in mechanism associated with photoproduct formation of I and II. At low $[\text{MK}^0]$, $\Phi_I \gg \Phi_{II}$, solvent abstraction reactions or photoreduction of the ketone are predominate (pinacol formation). At high $[\text{MK}^0]$, $\Phi_{II} \gg \Phi_I$, cross dimerization is favored as well as the appearance of increased absorption at long wavelengths upon continued irradiation. As irradiation is continued several deactivation processes are favored and the quantum yield drops in a predictable manner as shown in Figure 11, while absorbing photoproducts compete with MK for light absorption.[24,30,31]

The chemical nature of the solvents used in photoreactions of MK and DEABP is very important. Quantum yields for destruction of MK are $\Phi \simeq 0.4$, $[\text{MK}^0] = 1.2 \times 10^{-5}$ M in cyclohexane and $\Phi < 10^{-4}$, $[\text{MK}^0] = 5 \times 10^{-5}$ M in ethanol. The reason for this difference in photoreactivity or solvent dependence of aminoaromatic ketones lies in the fact that charge transfer (CT) spectra are influenced by the polarity of the

solvent. Other factors are reversal of n → π* and CT states, competition with singlet state deactivation, and hydrogen bonding to the carbonyl oxygen causing a change in ground state geometry.[30,31]

The shift in λ_{max} for MK in various solvents[30] correlates with the physical properties of the solvent such as refractive index (n^{25}D) and weight fraction of heteroatom in the solvent (χ).[32] The shift factor E (10^{-3} cm^{-1}) is given by

$$E = -6.43n^{25}\mathrm{D} - 4.77\chi + 38.89 \quad (43)$$

with a multiple correlation coefficient of 0.94. Similar solvent shifts to longer wavelengths with increasing polarity are also observed with DEABP.[32]

Primary Radical Termination in the Presence of MMA. The photochemistry of MK and by analogy DEABP suggests that both R_1· and R_2· might be effective initiating or terminating radicals for photopolymerization reactions. The following is a proposed scheme to account for the observed kinetic rate data in the photopolymerization of MMA with DEABP as photoinitiator:

$$[\text{triplet eximer}] \xrightarrow{K_r} R_1\cdot + R_2\cdot \text{ (primary radical formation)} \quad (44)$$

$$[\text{DEABP}^3] + ZH \xrightarrow{K_s} R_2\cdot \text{ (solvent abstraction)} \quad (45)$$

$$R_1\cdot + M \xrightarrow{K_{i_1}} R_1P\cdot \text{ (primary radical initiation)} \quad (46)$$

$$R_2\cdot + M \xrightarrow{K_{i_2}} R_2P\cdot \text{ (possible initiation)} \quad (47)$$

termination:

$$R_2\cdot + R_2\cdot \xrightarrow{Kt_1} \text{(pinacol formation)} \quad (48)$$

$$R_1\cdot + R_2\cdot \xrightarrow{Kt_2} \text{(cross dimerization)} \quad (49)$$

$$R_1\cdot + P\cdot \xrightarrow{Kt_3} \text{(primary radical termination)} \quad (50)$$

$$R_2\cdot + P\cdot \xrightarrow{Kt_4} \text{(growing polymer radical termination)} \quad (51)$$

$$P\cdot + P\cdot \xrightarrow{Kt_5} \text{(bimolecular termination)} \quad (52)$$

$$P\cdot + M \xrightarrow{K_p} \text{(polymer formation)} \quad (53)$$

A simplifying assumption to the above scheme is that R_2· does not cause initiation (K_{i_2} is not important) and can only undergo recombination (Kt_1), cross dimerization (Kt_2), and growing polymer radical termination (Kt_4). These modes of deactivation for R_2· are analogous with previously published work on the photopolymerization of MMA using benzophenone derivatives or anthraquinone as photoinitiators.[12,33] In these studies the reduced form of the ketone (semipinacol radical) did not initiate polymerization but only formed photoproducts or underwent termination with growing polymer radicals.

$$Ph_2C{=}O \xrightarrow{I_{abs}\phi_{st}} [Ph_2C{=}O]^3 \quad (54)$$

$$Ph_2C{=}O]^3 + ZH \rightarrow Ph_2\dot{C}\text{–}OH + Z\cdot \quad (55)$$

(semipinacol radical) (initiating radical)

$$Ph_2\dot{C}\text{–}OH + M \rightarrow \text{(possible initiation)} \quad (56)$$

$$2Ph_2\,\dot{C}\text{–}OH \rightarrow \text{(pinacol formation)} \quad (57)$$

$$P\cdot + Ph_2\,\dot{C}\text{–}OH \rightarrow \text{(termination)} \quad (58)$$

These modes of termination account for lower molecular weights of polymer formed during photopolymerization. Further detailed investigation of semipinacol initiation of monomers showed that at higher monomer concentrations (greater than 2 M) the ketyl radical can interact (rate of interaction with MMA 9×10^3 M^{-1} s^{-1}). Since rate constants for primary radical initiation are not known, this ketyl radical–MMA interaction could be insignificant by comparison.[34] If the semipinacol radical does initiate MMA then the rate for pinacol formation will be significantly decreased.

Case I. In the simplest approximation one can assume all initiation and termination is effected with only R_1· or that initiation is attributed to R_1· (R_1· + M >>> R_2· + M) and polymer radical (P·) termination is with R_2· and that R_1· termination = R_2· termination or both R_1· and R_2· are indistinguishable. These simple assumptions also neglect cross-dimerization (photoproduct formation) reactions (Kt_2). Therefore,

$$\frac{d[R_1\cdot]}{dt} = [\text{triplet eximer}]K_r - [R_1\cdot][M]K_{i_1} - [R_1\cdot][P\cdot]Kt_3 - [R_1\cdot][R_2\cdot]Kt_2 \quad (59)$$

Applying the steady state assumption to eq 59 and using eq 32 leads to

$$0 = \frac{d[R_1\cdot]}{dt} = \frac{I_{abs}\phi_{st}[\text{DEABP}^0]K_eK_r}{(K_r + K_d')(K_d + [\text{DEABP}^0]K_e + [ZH]K_s + [Q]K_q)} - [R_1\cdot]([M]K_{i_1} + [P\cdot]Kt_3 + [R_2\cdot]Kt_2) \quad (60)$$

Neglecting Kt_2, K_s, and K_q leads to

$$[R_1\cdot]([M]K_{i_1} + [P\cdot]Kt_3) = \frac{I_{abs}\phi_{st}[\text{DEABP}^0]K_eK_r}{(K_r + K_d')(K_d + [\text{DEAPB}^0]K_e)} \quad (61)$$

and assuming K_d is very small, 3×10^5 compared with K_e values of 10^{10} (ref 25), the final expression for $[R_1\cdot]$ is obtained

$$[R_1\cdot] = \frac{I_{abs}\phi_{st}K_r}{([M]K_{i_1} + [P\cdot]Kt_3)(K_r + K_d')} \quad (62)$$

The change in polymer radical formation is given by

$$\frac{d[P\cdot]}{dt} = [R_1\cdot][M]K_{i_1} - [R_1\cdot][P\cdot]Kt_3 - 2[P\cdot]^2Kt_5 \quad (63)$$

Substitution of eq 62 into eq 63 leads to

$$\frac{d[P\cdot]}{dt} = \frac{I_{abs}\phi_{st}K_r[M]K_{i_1}}{([M]K_{i_1} + [P\cdot]Kt_3)(K_r + K_d')} - \frac{I_{abs}\phi_{st}K_r[P\cdot]Kt_3}{([M]K_{i_1} + [P\cdot]Kt_3)(K_r + K_d')} - 2[P\cdot]^2Kt_5 \quad (64)$$

Application of the steady state assumption to [P·] leads to the following expression for [P·].

$$\{2[P\cdot]^2Kt_5\}([M]K_{i_1} + [P\cdot]Kt_3)(K_r + K_d') = I_{abs}\phi_{st}K_r[M]K_{i_1} - I_{abs}\phi_{st}K_r[P\cdot]Kt_3 \quad (65)$$

$$[P\cdot]^3 + \frac{[P\cdot]^2K_{i_1}[M]}{Kt_3} + \frac{I_{abs}\phi_{st}K_r[P\cdot]}{2Kt_5(K_r + K_d')} = \frac{I_{abs}\phi_{st}K_r[M]K_{i_1}}{2Kt_5Kt_3(K_r + K_d')} \quad (66)$$

This cubic equation can be simplified by replacing [P·] by $R_p/[M]K_p$ since $K_p[P\cdot][M] = R_p = -d[M]/dt$ (ref 35). Then eq 66 can be expressed as a cubic directly in terms of R_p.

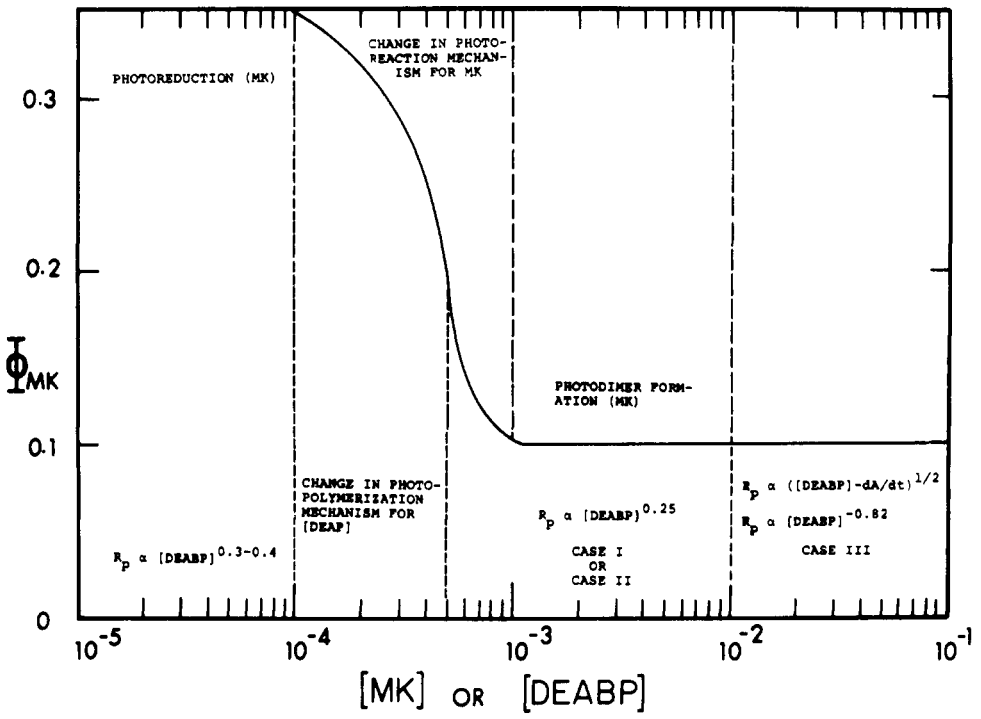

Figure 12. Rate of photopolymerization dependence on the initiator order for [DEABP] as compared with analogous concentration dependence of the quantum yield (Φ) for disappearance of [MK] in cyclohexane.[30]

$$R_p^3 + \frac{R_p^2 K_{i_1}[M]^2 K_p}{Kt_3} + \frac{I_{abs}\phi_{st}K_r R_p K_p^2[M]^2}{2Kt_5(K_r + K_d')} = \frac{I_{abs}\phi_{st}K_r K_{i_1} K_p^3[M]^4}{2Kt_5 Kt_3(K_r + K_d')} \quad (67)$$

If terms in R_p^2 and R_p in eq 67 are neglected and utilizing the relationship

$$I_{abs}\phi_{st} = I_0 \epsilon \phi_{st}[DEABP^0] \quad (68)$$

then the relationship between the rate of polymerization and I_0, [M] = [MMA], and [DEABP^0] can be expressed as

$$R_p \propto I_0^{1/3}[DEABP^0]^{1/3}[MMA]^{4/3} \quad (69)$$

This simple expression is consistent with the actual experimentally determined rates of photopolymerization and order of dependence on light intensity, monomer concentration, and initiator concentration as shown in eq 7. More specifically for the case I with the concentration range of initiator $1.5 \times 10^{-4} \leq [DEABP^0] \leq 5 \times 10^{-3}$, the experimental orders of light intensity, initiator concentration, and monomer concentration are 0.44, 0.25, and 1.35, respectively, which are in good agreement with the simplified theoretical expression shown in eq 69 within experimental errors.

Case II. If one assumes $R_2\cdot$ can initiate monomers with equal efficiency as $R_1\cdot$ at [M] = 9.28 M and neglecting combination reactions Kt_1 and Kt_2 or solvent effects (K_s) then

$$[R_1\cdot] = \frac{I_{abs}\phi_{st}K_r}{([M]K_{i_1} + [P\cdot]Kt_3)(K_r + K_d')} \quad (70)$$

and

$$[R_2\cdot] = \frac{I_{abs}\phi_{st}K_r}{([M]K_{i_2} + [P\cdot]Kt_4)(K_r + K_d')} \quad (71)$$

then

$$\frac{d[P\cdot]}{dt} = [R_1\cdot][M]K_{i_1} + [R_2\cdot][M]K_{i_2} - [R_1\cdot][P\cdot]Kt_3 - [R_2\cdot][P\cdot]Kt_4 - 2[P\cdot]^2 Kt_5 \quad (72)$$

Postulating that $K_{i_1} = K_{i_2}$, $Kt_3 = Kt_4$ leads to

$$\frac{d[P\cdot]}{dt} = \frac{2I_{abs}\phi_{st}K_r[M]K_{i_1}}{([M]K_{i_1} + [P\cdot]Kt_3)(K_r + K_d')} - \frac{2I_{abs}\phi_{st}K_r[P\cdot]Kt_3}{([M]K_{i_1} + [M]Kt_3)(K_r + K_d')} - 2[P\cdot]^2 Kt_5 \quad (73)$$

This equation has a similar solution as shown for case I as indicated by eq 69.

The overall rates of photopolymerization using this initiator DEABP are assumed to parallel the analogous concentration dependence of quantum yields for photochemical disappearance of MK. This is schematically summarized in Figure 12. The changes in mechanism associated with radical production of photoproducts for MK are also solvent and concentration dependent as are similar reaction pathways proposed for DEABP.

At DEABP concentration ranges of 0.5×10^{-5} to 10×10^{-5} M the kinetics order for initiator is in the region of 0.3 to 0.4 (close to the 0.5 order in initiator for ideal systems) but at higher concentration ranges ([DEABP] = 1.5×10^{-4} M) the rate of photopolymerization is proportional to the 0.23–0.25 order in initiator. At low sensitizer concentrations there is less chance for primary radical interaction with the growing polymer radical and normal modes of termination are more important. The actual termination steps are probably mixtures of mostly normal and, to a lesser extent, primary radical combination. At [DEABP] $\geq 1.5 \times 10^{-4}$ M primary radical termination is important and solving the cubic equation is necessary to account for the apparent loss in initiating efficiency of the primary radical. At low photoinitiator concentrations the photochemical reduction of [DEABP^3] with MMA or PMMA as the only solvent or chain transfer medium to form $R_2\cdot$ and pinacol photoproducts is probably not significant.

Case III. At very high concentrations of DEABP (1 to 6×10^{-2} M) there was noticed formation of a yellow collored intermediate (photoproduct) accompanied by a decrease in rate of polymerization at increasing DEABP concentrations.

A plot of absorbance vs. wavelength for the colored photo-

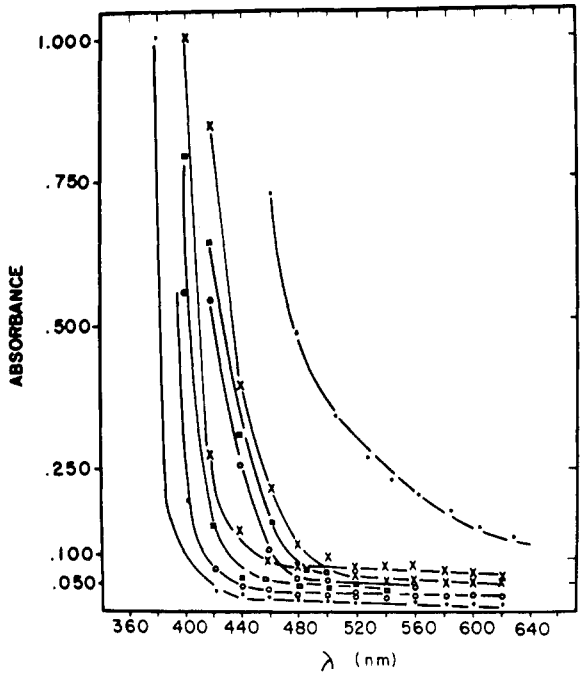

Figure 13. Plot of absorbance against wavelength (nm) for the formation of colored photoproducts time (t) = 0 and 40 min exposure to ultraviolet irradiation: (●) 6×10^{-2} M DEABP in benzene; (○) 1×10^{-2} M DEABP in MMA; (□) 3×10^{-2} M DEABP in MMA; (X) 6×10^{-2} M DEABP in MMA.

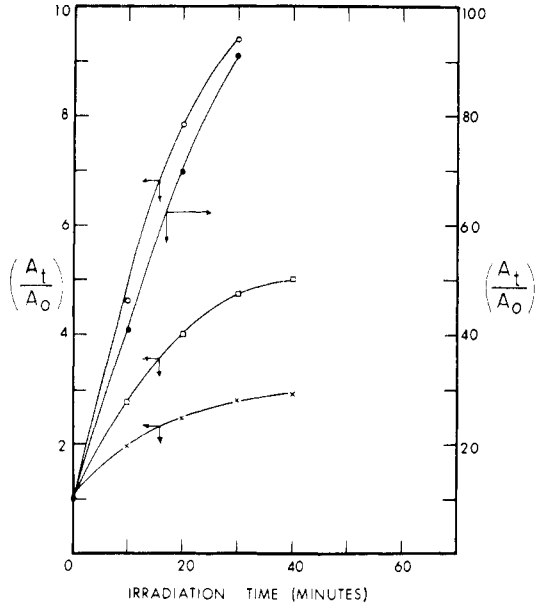

Figure 14. Relative rates of change in absorbance (At/A_0) at 440 nm as a function of irradiation time: [DEABP] = 6×10^{-2} M in benzene (●), 1×10^{-2} M in MMA (○), 3×10^{-2} M in MMA (□), and 6×10^{-2} M in MMA (X).

products produced during DEABP photoinitiated polymerization of MMA and photoreactions of DEABP in benzene is shown in Figure 13.

Figure 14 gives the relative rates of change in absorbance at 440 nm as a function of irradiation time. The rates of photopolymerization and relative changes in absorption (dA/dt) are equivalent, as shown in Figure 15, and both show reciprocal dependence in DEABP concentration shown in Figure 16. In benzene when there is no photopolymerization taking place and using up or competing with the initial primary radical production, the formation of the yellow photoproduct

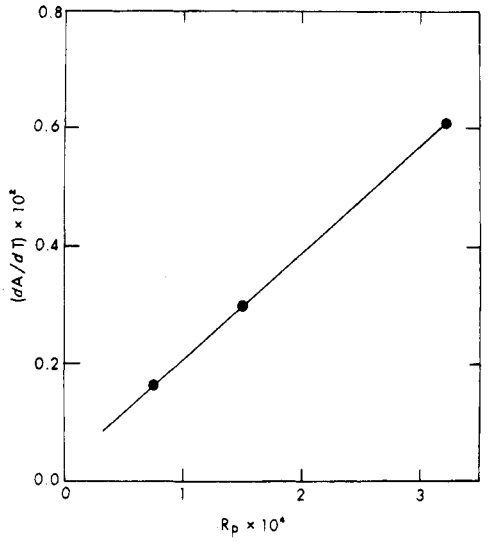

Figure 15. A plot of the slopes from Figure 14 [relative changes in absorption (dA/dt)] at λ = 440 nm vs. rate of polymerization (R_p).

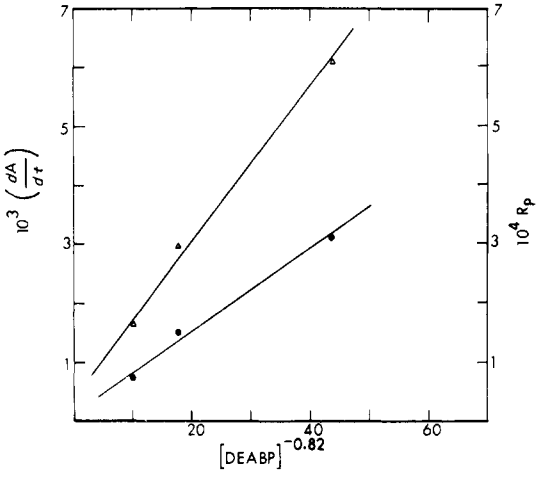

Figure 16. Reciprocal dependence of R_p and (dA/dt) on [DEABP].

is quite significant. Similar yellow colored photoproducts have been reported for the irradiation of MK in benzene.[7]

$$\text{DEABP} \xrightarrow{I_{abs}\phi_{st}} R_1\cdot + R_2\cdot \begin{cases} \xrightarrow{\text{benzene}} \text{photoproducts} \\ \xrightarrow{\text{MMA}} \text{polymer and photoproducts} \end{cases} \quad (74)$$

A possible explanation for these results is that at high initiator concentrations the relative rates of photoproduct formation compete successfully with primary radical initiation and possibly growing polymer radical termination.

$$\text{DEABP} \xrightarrow{I_{abs}\phi^{st}} R_1\cdot + R_2\cdot \quad (75)$$

$$R_1\cdot + M \xrightarrow{K_{i_1}} P\cdot \quad (76)$$

$$R_2\cdot + R_2\cdot \xrightarrow{Kt_1} \text{[pinacol; not a long wavelength 350–500 nm photoproduct } (\lambda_{max} \text{ 265 nm, } \epsilon = 15\,000)] \quad (77)$$

$$R_1\cdot + R_2\cdot \xrightarrow{Kt_2} \text{(photoproduct; possibly responsible for, observed long wavelength absorption concurrent with the rate of photopolymerization)} \quad (78)$$

$$R_1\cdot + P\cdot \xrightarrow{Kt_3} \text{(primary radical; polymer radical termination)} \quad (79)$$

$$P\cdot + P\cdot \xrightarrow{Kt_5} \text{(normal termination)} \quad (80)$$

$$P\cdot + M \xrightarrow{K_p} \text{(propagation)} \quad (81)$$

$$R_1\cdot \text{ or } R_2\cdot + \text{DEABP} \xrightarrow{Kt_6} \text{long wavelength photoproducts} \quad (82)$$

Ignoring Kt_3 and Kt_1 the following rate equations are obtained for $R_1\cdot$ and $P\cdot$

$$d[R_1\cdot]/dt = I_{abs}\phi_{st} - [R_1\cdot][M]K_{i_1} - [R_1\cdot][R_2\cdot]Kt_2 \quad (83)$$

$$d[P\cdot]/dt = [R_1\cdot][M]K_{i_1} - 2[P\cdot]^2 Kt_5 \quad (84)$$

Since $[P\cdot] = R_p/[M]K_p$ and

$$dA/dt = [R_1\cdot][R_2\cdot]Kt_2 \quad (85)$$

(change in absorbance for photoproduct formation)

applying steady state conditions to eq 83 and 84 for $[R_1\cdot]$ and $[P\cdot]$, respectively, leads to the final expression for R_p.

$$R_p = \left(\frac{I_{abs}\phi_{st} - dA/dt}{2Kt_5}\right)^{1/2}[M]K_p \quad (86)$$

A plot of R_p vs. $(I_{abs}\phi_{st} - dA/dt)^{1/2}$ is linear with a 0.99 correlation and is shown in Figure 17. This is consistent with all initiating radicals forming photoproducts or being intercepted by monomer and not available for primary radical termination with growing polymer radicals.

At high DEABP concentrations, the optical density of the reaction cell is very large at the side wall causing the radiation absorption layer to be small and could result in decreasing R_p at increasing [DEABP] as well as unusual kinetic orders in light intensity. Under these conditions dimerization to photoproducts might be predominant or internal screening effects (shift to longer wavelength photoproducts or self quenching) could account for the observed results.[30,31,34,36]

$R_1\cdot \xrightarrow{M,\ K_{i_1}P\cdot}$ initiation; $\xrightarrow{Kt_3}$ primary radical termination } low to intermediate DEABP concentration (87)

$R_1\cdot \xrightarrow{Kt_2} R_2\cdot$

$R_1\cdot \text{ or } R_2\cdot \xrightarrow[Kt_6]{\text{DEABP}}$ photoproducts (long wavelength) } high DEABP concentration (88)

Another possible explanation for the increased yellow photoproduct formation might be attributed to quinol structures

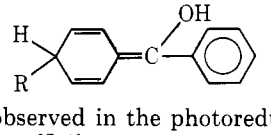

similar to those observed in the photoreduction of benzophenone/benzhydrol.[37–40] This type of radical addition reaction can be represented by Kt_6.

Primary Radical Termination. The following, somewhat different, kinetic scheme was utilized by Ledwith[12,33] to account for termination of growing polymer radicals with ketyl or anthraquinone radicals ($R_2\cdot$):

$$P\cdot + (Ar)_2\dot{C}{-}OH \xrightarrow{Kt'} P{-}C(Ar)_2{-}OH \quad (89)$$

($R_2\cdot$)

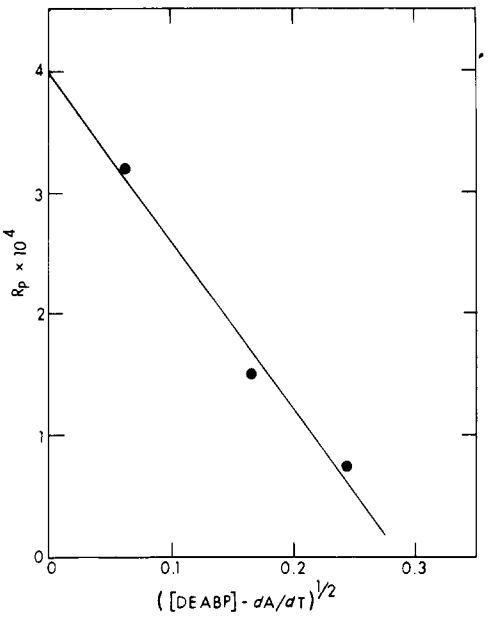

Figure 17. Correlation between R_p and $([DEABP] - dA/dt)^{1/2}$.

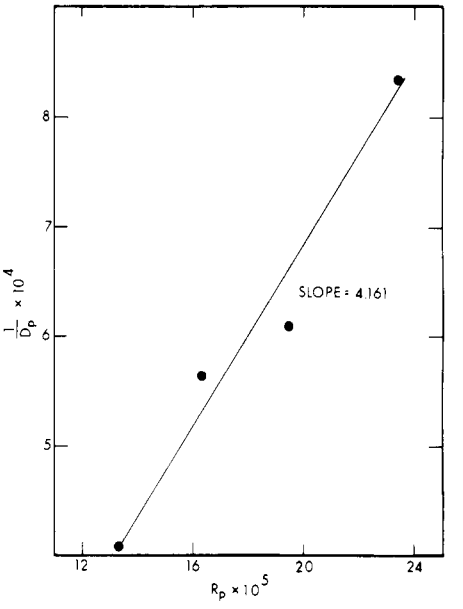

Figure 18. Plot of $1/D_p$ vs. R_p for the photopolymerization of MMA with DEABP photoinitiator [DEABP] = 5 to 50 × 10^{-4} M.

$$P\cdot + P\cdot \xrightarrow{Kt} P{-}P \quad (90)$$

$$(Ar)_2\dot{C}{-}OH + (Ar)_2\dot{C}{-}OH \xrightarrow{K_c} \text{pinacol formation} \quad (91)$$

$$[P\cdot] = \frac{(I_{abs}\phi_{st})^{1/2}[Ar_2CO]}{Kt^{1/2}(1+\alpha)^{1/2}} \quad (92)$$

where

$$\alpha = Kt'/(KtK_c)^{1/2} \quad (93)$$

A graph of $1/D_p$ vs. R_p for the photopolymerization of MMA with DEABP is shown in Figure 18 (correlation coefficient 0.98) and the slope of this plot is a measure of $K_p/Kt^{1/2}$.[41–43] Comparison of $K_p/Kt^{1/2}$ for DEABP–MMA with data taken from ref 12 and 33 for photopolymerization of MMA with benzophenone, anthraquinone, and azodiisobutyronitrile (VAZO-64) is given in Table V. In the ideal case (VAZO-64, no primary radical–polymer radical termination) $K_p/Kt^{1/2}$ values are approximately 0.0658 and $\alpha = 0$. The DEABP–

Table V
Photopolymerization of MMA at 30 °C

Sensitizer	$K_p/Kt^{1/2}(1+\alpha)^{1/2}$	$\alpha = Kt'/(KtK_c)^{1/2}$	Ref
Benzophenone	0.0306	3.62	12
3,3′,4,4′-Tetramethoxycarbonylbenzophenone (TMCB)	0.0404	1.65	12
3,3′,4,4′-Benzophenonetetracarboxylic dianhydride (BTDA)	0.0559	0.39	12
Anthraquinone	0.043	1.35	33
VAZO-64	0.0658	0	26
DEABP	0.0528	0.55	This work

Table VI
Solvent Effects on the Photopolymerization of MMA Using DEABP as the Photoinitiator[a]

Solvent MMA	% monomer converted/s
Benzene	3×10^{-3}
Cyclohexane	1×10^{-4}
Methanol	No polymer formed

[a] [DEABP] = 1×10^{-3} M.

MMA values for $K_p/Kt^{1/2}$ are 0.0528 and are similar to those of the substituted benzophenones. This lowering of the molecular weights is not an effect of direct ground state molecular abstraction since R_p and polymer molecular weights under thermal conditions (VAZO-64 + DEABP) showed no signs of abnormal rate change or photoinitiator uptake during the thermal reaction as indicated in Figure 5 and Table III. The reduction in molecular weight is consistent with free-radical intermediates formed during the initiation process that lead to growing polymer radical termination reactions.

Solvent Effects. Michler's ketone derivatives are known to have large wavelength absorption shifts in solvents of different polarity and the photodestruction of MK in solution also depends upon the chemical structure of the solvent. Irradiation of MK in cyclohexane ($\phi_{st} = 0.91$) results in photoreduction to the pinacol and is concentration dependent; benzene solvents ($\phi_{st} = 1.00$) result in photodimer products having long wavelength absorptions and alcohol solvents ($\phi_{st} = 0.08$) show little photochemical reactivity.[30,31]

Table VI shows the dramatic effect of solvent interaction on the rate and mechanism of photopolymerization of MMA/solvent at constant [DEABP] = 1×10^{-3} M. In MMA/benzene, primary radical initiation without competitive reduction results in large amounts of polymer formation (3×10^{-3}% monomer converted/s). In MMA/cyclohexane the mechanistic pathway is photoreduction without primary initiating radical formation resulting in very low amounts of polymer formation (1×10^{-4}% monomer converted/s). Photoreactions in alcohol solvents MMA/methanol resulted in no polymer formation.

These results indicate that $R_2\cdot$ formed under the above conditions do not appear to initiate MMA as effectively as $R_1\cdot$ (primary initiating radical species).

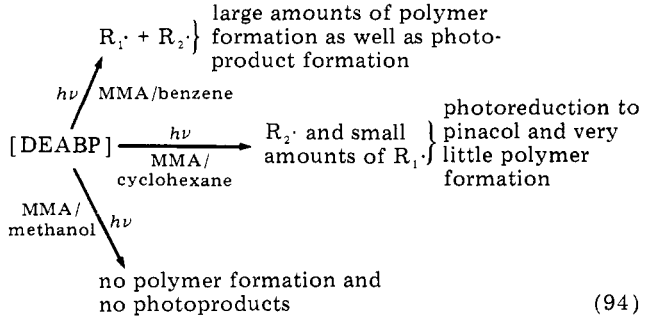

(94)

In conclusion, the photochemistry of aminoaromatic ketones is complicated by self-quenching reactions, concentration, and solvent effects. These photophysical properties for aminoaromatic ketones are reflected in unusual kinetic behavior on rates of polymerization of MMA and efficiency for photogeneration of an initiating free-radical species.

Acknowledgments. Part of this work performed by A. Gallopo was supported by a National Science Foundation "Faculty Research Participation" grant having Proposal/Grant No. Ser-76-04704.

References and Notes

(1) (a) Address correspondence to this author at Battelle Columbus Laboratories; (b) Montclair State College.
(2) (a) M. N. Giangualano et al., U.S. Patent 3 376 138–9 (1968); (b) C. Teh-Lin Chang, U.S. Patent 3 661 588 (1972).
(3) J. F. Ackerman et al., U.S. Patent 3 673 140 (1972).
(4) V. D McGinniss, U.S. Patents 3 847 771 (1974) and 3 878 075 (1975).
(5) C. C. Wamser et al., *J. Am. Chem. Soc.*, **92,** 6362 (1970).
(6) T. H. Koch and A. H. Jones, *J. Am Chem. Soc.*, **92,** 7503 (1970).
(7) D. I. Schuster and M. D. Goldstein, *J. Am. Chem. Soc.*, **95,** 986 (1973).
(8) S. P. Pappas and A. Chattopadhyay, *J. Am. Chem. Soc.*, **95,** 6484 (1973).
(9) J. F. Rabek, "The Sensitizing Effects of Benzophenone and Michler's Ketone in Photochemistry of Polymers", Technical Papers, "RETEC in Photopolymers", Society of Plastics Engineers, Inc., Ellenville, N.Y., October 24–26, 1973.
(10) B. Ranby and J. F. Rabek, "Photodegredation, Photo-oxidation and Photostabilization of Polymers," Wiley, New York, N.Y., 1975.
(11) V. D. McGinniss, *ACS Symp. Ser.*, **No. 25,** 135 (1976).
(12) H. Block, A. Ledwith, and A. R. Taylor, *Polymer*, **12,** 271 (1971).
(13) W. H. Moore, G. S. Hammond, and R. P. Foss, *J. Am. Chem. Soc.*, **83,** 2789 (1961).
(14) T. Provder, "Analysis of Copolymers by GPC", presented at 58th Canadian Chemical Conference, Macromolecular Science Division, May 6, 1975.
(15) T. Provder and C. Kuo, *Org. Coatings Plastics Chem. Prepr.*, **36 (2),** 7 (1976).
(16) D. D. Bly, *J. Polym. Sci., Part C*, **21,** 13 (1968).
(17) Z. Grubisic, P. Rempp, and H. Benoit, *J. Polym. Sci., Part B*, **5,** 753 (1967).
(18) T. Provder, J. C. Woodbery, J. H. Clark, and E. E. Drott, *Adv. Chem. Ser.*, **125,** 117 (1973).
(19) H. Coll, and L. R. Prusinowski, *J. Polym. Sci., Part B*, **5,** 1153 (1967).
(20) H. J. Cantow, J. Pouyet, and C. Wippler, *Makromol. Chem.*, **14,** 110 (1954).
(21) H. J. Cantow and G. V. Schulz, *Z. Phys. Chem. (Frankfurt am Main)*, **2,** 117 (1954).
(22) T. Provder and E. M. Rosen, *Sep. Sci.*, **5,** 437 (1970).
(23) L. H. Tung, *J. Appl. Polym. Sci.*, **10,** 375 (1966).
(24) V. D. McGinniss and D. M. Dusek, *Polym. Prepr., Am. Chem. Soc., Div. Polym. Chem.*, **15 (1),** 480 (1974).
(25) V. D. McGinniss and D. M. Dusek, *J. Paint Technol.*, **46 (589),** 23 (1974).
(26) C. H. Bamford et al., "The Kinetics of Vinyl Polymerization by Radical Mechanisms", Butterworths, London, 1958.
(27) G. E. Scott and E. Senogles, *J. Macromol. Sci., Chem.*, **8 (4),** 753 (1974).
(28) G. E. Scott and E. Senogles, *J. Macromol. Sci., Rev. Macromol. Chem.*, **9 (1),** 49 (1973).
(29) P. E. M. Allen and C. R. Patrick, *Makromol. Chem.*, **48,** 89 (1961).
(30) P. Suppan, *J. Chem. Soc., Faraday Trans. 1*, **71 (3),** 539 (1975).
(31) D. I. Schuster, M. D. Goldstein, and P. Bane, *J. Am. Chem. Soc.*, **99,** 187 (1977).
(32) V. D. McGinniss, unpublished results.
(33) A. Ledwith, G. Ndaaliv, and A. R. Taylor, *Macromolecules*, **8 (1),** 1 (1975).
(34) R. Kuhlman and W. Schuabel, *Angew. Makromol. Chem.*, **57,** 195 (1977).
(35) C. H. Bamford, A. D. Jenkins, and R. Johnston, *Trans. Faraday Soc.*, **55,** 1451 (1959).
(36) R. Srinivason and T. D. Roberts, "Organic Photochemical Synthesis", Vol. 1, Wiley-Interscience, New York, N.Y., 1971.
(37) S. G. Cohen and J. I. Cohen, *Tetrahedron Lett.*, 4823 (1968).
(38) S. G. Cohen and J. I. Cohen, *Isr. J. Chem.*, **6,** 757 (1968).
(39) N. Filipescu and F. L. Minn, *J. Chem. Soc. B*, 84 (1969).
(40) H. L. J. Bäckström and R. J. V. Niklasson, *Acta Chem. Scand.*, **22,** 2589 (1968).
(41) G. P. Gladrshev and K. M. Gibov, "Polymerization at Advanced Degrees of Conversion", Israel Program for Scientific Translations, Wiener Binderg Ltd., Jerusalem, 1970.
(42) S. Sakai and K. Takahashi, *Polym. J.*, **6 (5),** 341 (1974).
(43) T. E. Ferington and A. V. Tobolsky, *J. Am. Chem. Soc.*, **77,** 4510 (1955).